Supporting Information

Oxygen Vacancy Defects Boosted High Performance p-Type Delafossite $CuCrO_2$ Gas Sensors

Bin Tong,[†,‡] Zanhong Deng,[†,§] Bo Xu,[⊥] Gang Meng,[†,§,*] Jingzhen Shao,[†,§] Hongyu Liu,[†,‡] Tiantian Dai,[†,‡] Xueyan Shan,[†,‡] Weiwei Dong,[†,§] Shimao Wang,[†,§] Shu Zhou,[†] Ruhua Tao,[†,§] Xiaodong Fang, [†,§,*]

[†]Anhui Provincial Key Laboratory of Photonic Devices and Materials, Anhui Institute of Optics and Fine Mechanics, and [§]Key Lab of Photovoltaic and Energy Conservation Materials, Chinese Academy of Sciences, Hefei 230031, China

[‡]University of Science and Technology of China, Hefei 230026, China.

[⊥]China Pharmaceutical University, Nanjing 211198, China.

Corresponding Author

*Email: menggang@aiofm.ac.cn

*Email: xdfang@aiofm.ac.cn

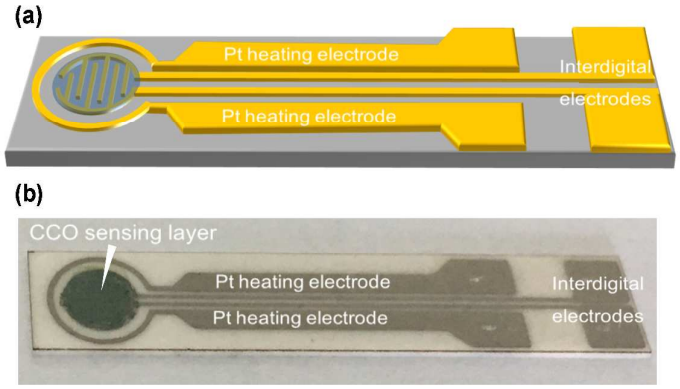

Figure S1. The schematic (a) and photograph (b) of the sensor devices.

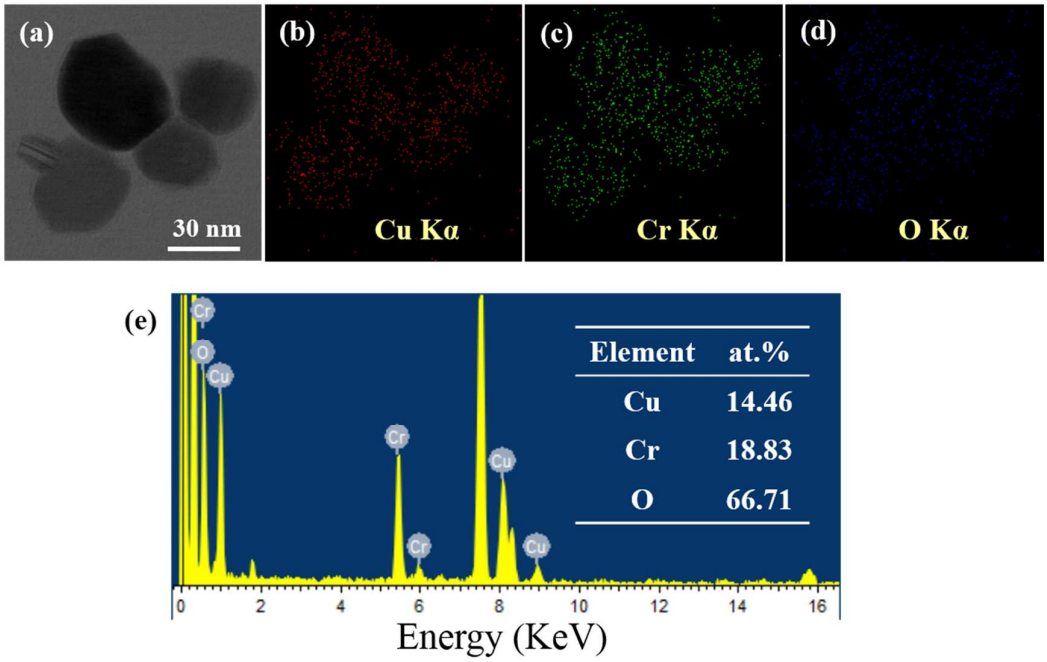

Figure S2. TEM EDS mapping (a)-(d) and EDS (e) results of g-CCO nanoparticles.

Figure S2 illustrates that Cu, Cr and O element were homogeneously distributed in the CCO nanoparticle. The atomic ratio of Cu (14.46 %) to Cr (18.83 %) is 0.77:1, inferring a deficiency of Cu in delafossite CCO nanoparticles.

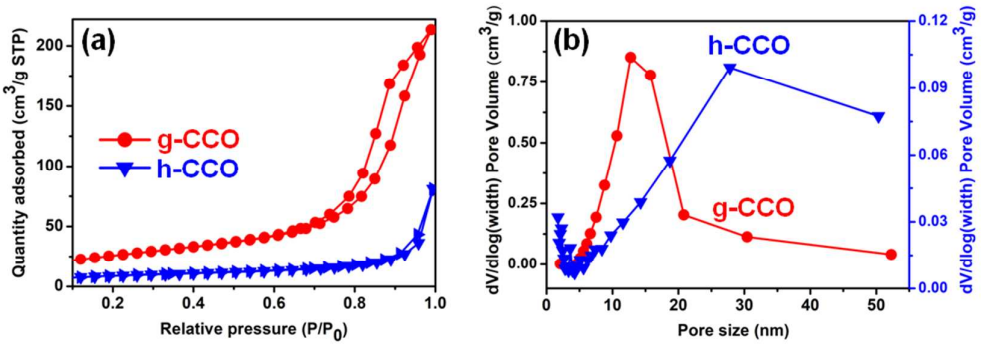

Figure S3. (a) BET nitrogen adsorption-desorption isotherms. (b) BET-pore size distribution of as-synthesized CCO nanoparticles.

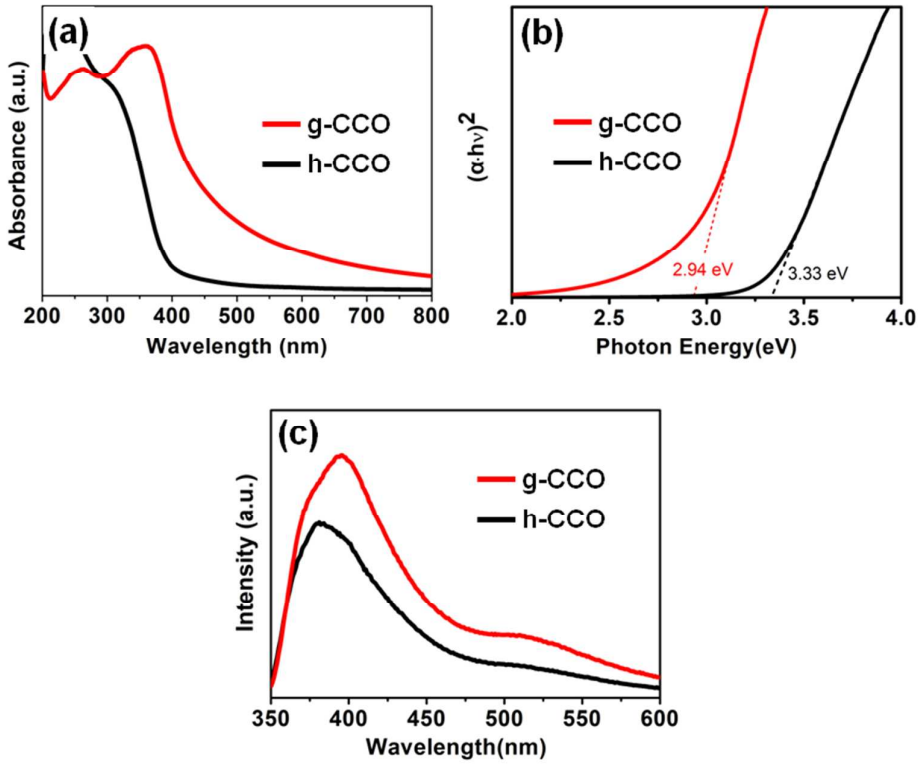

Figure S4. (a) UV-Vis absorption spectrum. (b) The corresponding $(\alpha h\nu)^2$ versus $h\nu$ plot, where α is the absorption coefficient, $h\nu$ is the photon energy. (c) Photoluminescence spectroscopy of CCO nanoparticles.

UV-Vis absorption spectroscopy (Figure S4a) demonstrates a clear difference in absorption edge of two kinds of CCO. h-CCO exhibits negligible absorbance in the

range of ~450 - 800 nm, while a abrupt increase of absorption coefficient in the UV range (< 400 nm). On the other hand, g-CCO obtained by glycine nitrate process shows a relatively high and broad absorption in the range of 450 - 800 nm. Since the relationship between the absorption coefficient and the band gap energy can be described by the formula: $(\alpha h\nu)^2 = A(h\nu - E_g)$, where $h\nu$ and E_g are photon energy and optical band gap energy, respectively, and A is the characteristic constant. We can estimate the band gap by extrapolation of the linear relation to $(\alpha h\nu)^2 = 0$, as shown in the Figure S4b. E_g of g-CCO and h-CCO are 2.94 eV and 3.33 eV, respectively, which is close to the reported literature value of 3.1 eV.[1] The smaller grain size of h-CCO may result in a blue shift of E_g. In line with absorption spectrum, a blue shift of band edge emission was observed for the h-CCO nanoparticles, as seen in the PL spectrum (excitation wavelength of 325 nm) in Figure S4c. In addition to band edge emission, a broad green emission band (centered at ~ 510 nm) was found in both samples, suggesting the presence of defect level within the band gap.

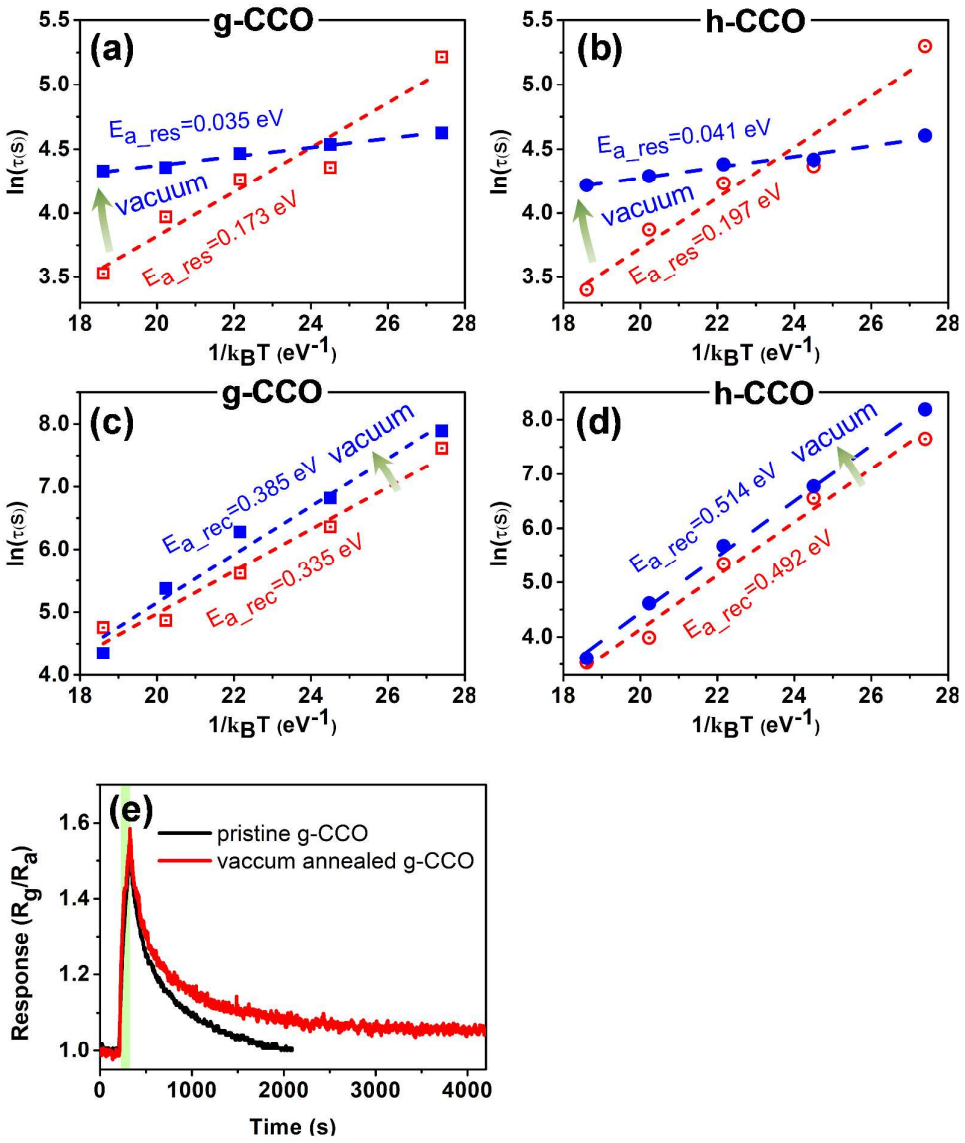

Figure S5. The derived activation energy of pristine and vacuum annealed CCO sensors for detecting 100 ppm ethanol, τ(s) is response/ recovery time. Response and recovery characteristics of CCO sensors. (a) Response activation energy of pristine and vacuum annealed g-CCO sensors. (b) Response activation energy of pristine and vacuum annealed h-CCO sensors. (c) Recovery activation energy of pristine and vacuum annealed g-CCO sensors. (d) Recovery activation energy of pristine and vacuum annealed h-CCO sensors. (e) The recovery characteristics of pristine and vacuum annealed g-CCO (toward 100 ppm ethanol, operation temperature is 150 ºC).

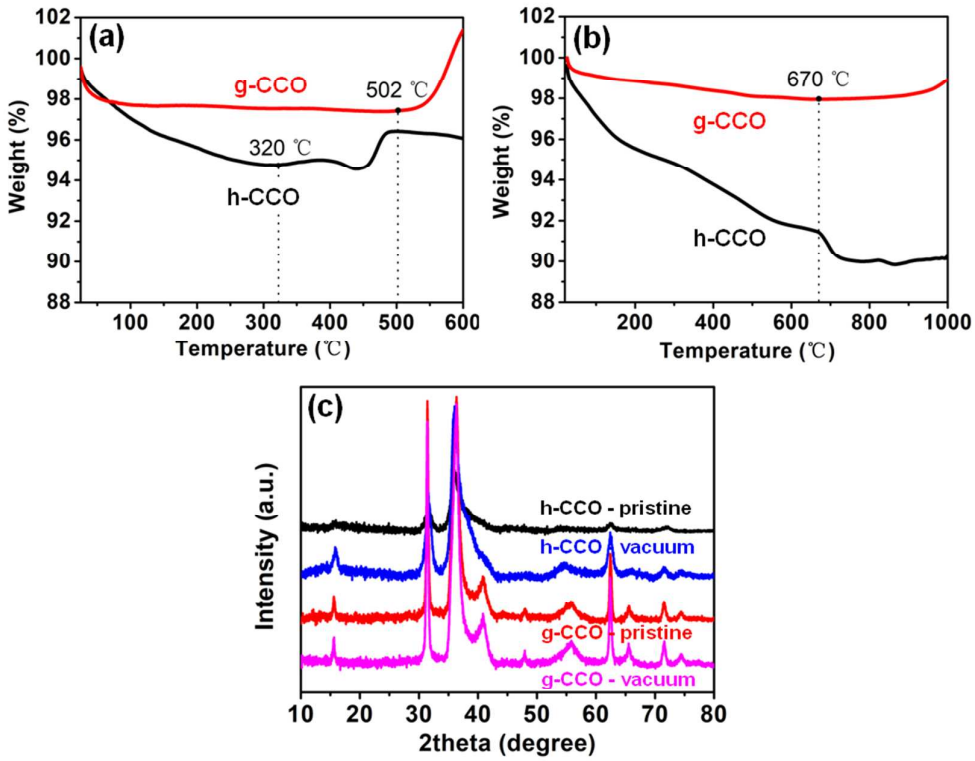

Figure S6. Thermal stability of as-synthesized CCO nanoparticles. (a) TGA curves of CCO nanoparticles in air atmosphere. (b) TGA curves of CCO nanoparticles in nitrogen atmosphere. (c) XRD patterns of CCO samples before and after vacuum annealing performed at 350 °C.

We have investigated the thermal stability of CCO nanoparticles both in air and nitrogen atmosphere. g-CCO nanoparticles prepared by glycine nitrate process possess a high thermal stability in both air (up to ca. 502 °C) and inert (nitrogen) atmosphere (up to ca. 670 °C), steming from a high temperature (ca. 900 – 1100 °C) self-combustion process in air atmosphere.[2] In contrast, the h-CCO nanoparticles prepared by hydrothermal method show a relative poor stability, especially in air atmosphere (up to ca. 320 °C, propably due to oxidation of Cu^{+} to Cu^{2+}, corresponding to a phase transition from $CuCrO_2$ to $CuCr_2O_4$)[3], as shown in Figure S6a and S6b. Thus, the operation temperature of CCO sensors were performed below 320 °C (in air atmosphere) in this work. Vaccum annealing treatment at 350 °C would not cause phase transition (Figure S6b and S6c) and any detectable grain size varision

estimated by Debye-Scherrer formula, ruling out the possibility of impurity or grain size induced sensitivity enhancement shown in Figure 5c.

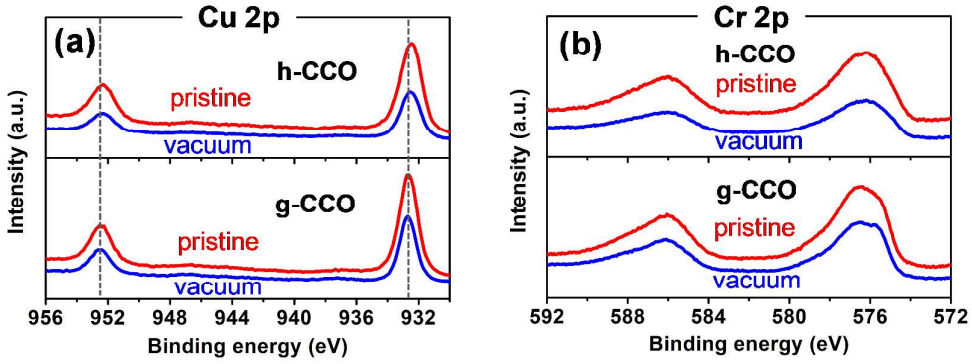

Figure S7. XPS Cu 1s (a) and Cr 1s (b) spectra of CCO sensors before and after vacuum annealing. Minor peak shift was induced by vacuum annealing.

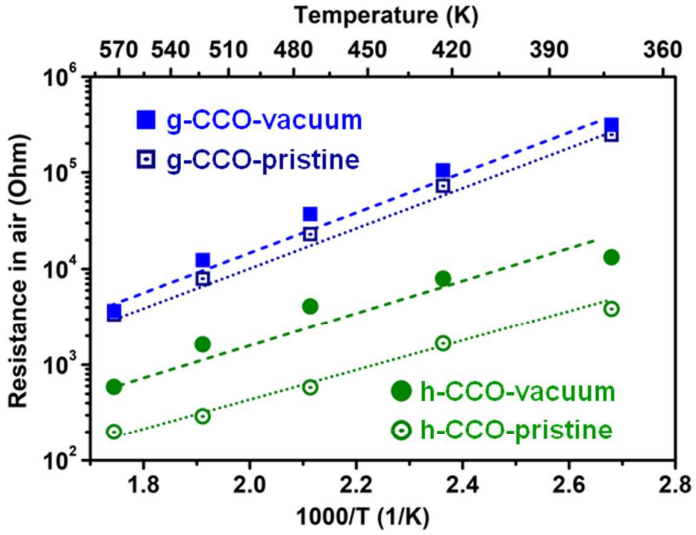

Figure S8. Temperature dependent resistance of CCO sensors. Vacuum annealing at 350 °C results in a resistance increase for both sensors.

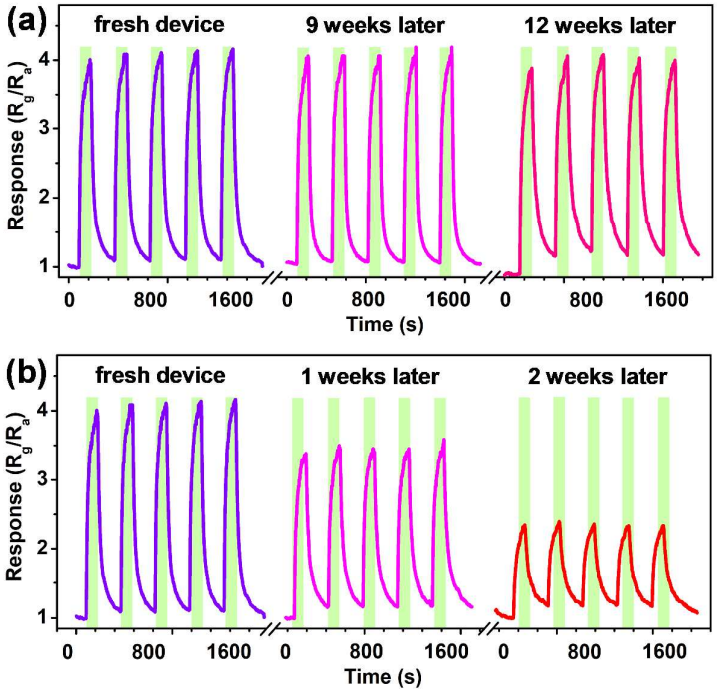

Figure S9. Stability test of Vo· rich g-CCO sensor (100 ppm ethanol, 300 ºC, 5 cycles). (a) Response curves under an 'incontinuous' test mode (the heating time was less ~5 h/week). (b) Response curves under an accelerated aging test (aging at 300 ºC in air, ~10 h/day).

References

(1) Deng, Z. H.; Fang, X. D.; Li, D.; Zhou, S.; Tao, R. H.; Dong, W. W.; Wang, T.; Meng, G.; Zhu, X. B. Room Temperature Ozone Sensing Properties of p-Type Transparent Oxide $CuCrO_2$. *J. Alloys Compd.* **2009**, *484,* 619-621.

(2) Nien, Y. T.; Hu, M. R.; Chiu, T. W.; Chu, J. S. Antibacterial Property of $CuCrO_2$ Nanopowders Prepared by a Self-Combustion Glycine Nitrate Process. *Mater. Chem. Phys.* **2016**, *179,* 182-188.

(3) Ursu, D.; Miclau, M. Thermal Stability of Nanocrystalline 3R-$CuCrO_2$. *J.Nanopart. Res.* **2013**, *16*, 2160-2166.